THE JOURNAL OF PHYSICAL CHEMISTRY B

Article

pubs.acs.org/JPCB

Crystal Structures of IAPP Amyloidogenic Segments Reveal a Novel Packing Motif of Out-of-Register Beta Sheets

Angela B. Soriaga,[†,‡,§,∥] Smriti Sangwan,[†,‡,§,∥] Ramsay Macdonald,[‡,∥] Michael R. Sawaya,[†,‡,§,∥] and David Eisenberg*[,†,‡,§,∥]

[†]Howard Hughes Medical Institute, [‡]UCLA-DOE Institute of Genomics and Proteomics, [§]Department of Biological Chemistry, and [∥]Department of Chemistry & Biochemistry, UCLA, Los Angeles, California 90095, United States

ABSTRACT: Structural studies of amyloidogenic segments by X-ray crystallography have revealed a novel packing motif, consisting of out-of-register β sheets, which may constitute one of the toxic species in aggregation related diseases. Here we sought to determine the presence of such a motif in islet amyloid polypeptide (IAPP), whose amyloidogenic properties are associated with type 2 diabetes. We determined four new crystal structures of segments within IAPP, all forming steric zippers. Most interestingly, one of the segments in the fibril core of IAPP forms an out-of-register steric zipper. Analysis of this structure reveals several commonalities with previously solved out-of-register fibrils. Our results provide additional evidence of out-of-register β sheets as a common structural motif in amyloid aggregates.

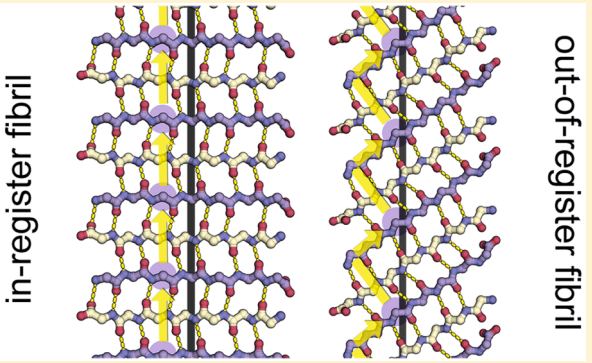

INTRODUCTION

Protein aggregation and its associated cytotoxicity are implicated in a wide range of diseases that affect the nervous system as well as other organs; recently protein aggregates have also been associated with certain forms of cancer.[1−4] Altogether these conditions account for the majority of diseases with few to no treatment options. One step toward understanding the disease etiology is to identify the molecular structures of the aggregated states of proteins that cause cellular dysfunctions. While the atomic structures of the spine of amyloid fibrils have been shown to be made up of β sheets with interdigitating side chains termed steric zippers,[5,6] scientists remain confounded about the structures of intermediates that are formed as amyloid proteins transition from monomeric states to insoluble aggregates. An additional complication is that aggregation of proteins yields a heterogeneous population of species that are difficult to separate and characterize. To date, researchers have identified multiple aggregated species, often termed polymorphs, that vary in size, secondary structure, and cytotoxicity, but there is as yet no consensus about the molecular structures of the toxic species in amyloid-related diseases.[7,8]

Recently, structural studies have revealed a novel packing motif, the antiparallel out-of-register β sheet, that may be associated with cytotoxicity in vitro. In one study, the crystal structure of an 11-residue segment from the amyloid protein αB Crystallin (ABC) was deciphered.[9] The structure, termed cylindrin, is a six-stranded β barrel made up of out-of-register antiparallel β strands. Cylindrin displayed a novel arrangement of β strands different from the steric zippers seen in amyloid fibrils. In most steric zippers, the strands in each β sheet are stacked directly above one another, an arrangement termed in-register; cylindrin instead has out-of-register strands that shear relative to strands below. The out-of-register strands of cylindrin form hexameric oligomers in solution, which were mildly cytotoxic to cells in vitro.[9]

In other studies, atomic structures of amyloid β-sheet mimics (BAMs) and a hexameric segment from β2-microglobulin (β2m) were determined showing the cylindrin-like feature of out-of-register β strands.[10−12] The short segment of β2m with the amino acid sequence KDWSFY formed an unusual out-of-register steric zipper. The segment was mildly cytotoxic to cultured cells in vitro, and it was suggested that the toxicity of out-of-register fibrils might derive from forming cylindrin-like oligomers. In view of these out-of-register structures, we set out to investigate if such a motif can be formed by segments of islet amyloid polypeptide (IAPP), the protein associated with type 2 diabetes.

IAPP is a 37-residue peptide secreted by the β-cells of the pancreas.[13,14] It is the main component of extracellular aggregates that display classic amyloid characteristics and are found in majority of patients suffering from type 2 diabetes.[15,16] The segment from residues 20−29 has been suggested to form the core of IAPP fibrils, as mutating this region blocks fibril formation.[17] Furthermore, mouse IAPP, which has several different residues in this region, does not aggregate and mice do not get diabetes. Another important aspect of IAPP aggregation is that the protein can adopt different conformations in its

Special Issue: William M. Gelbart Festschrift

Received: October 12, 2015
Revised: December 2, 2015

DOI: 10.1021/acs.jpcb.5b09981
J. Phys. Chem. B XXXX, XXX, XXX−XXX

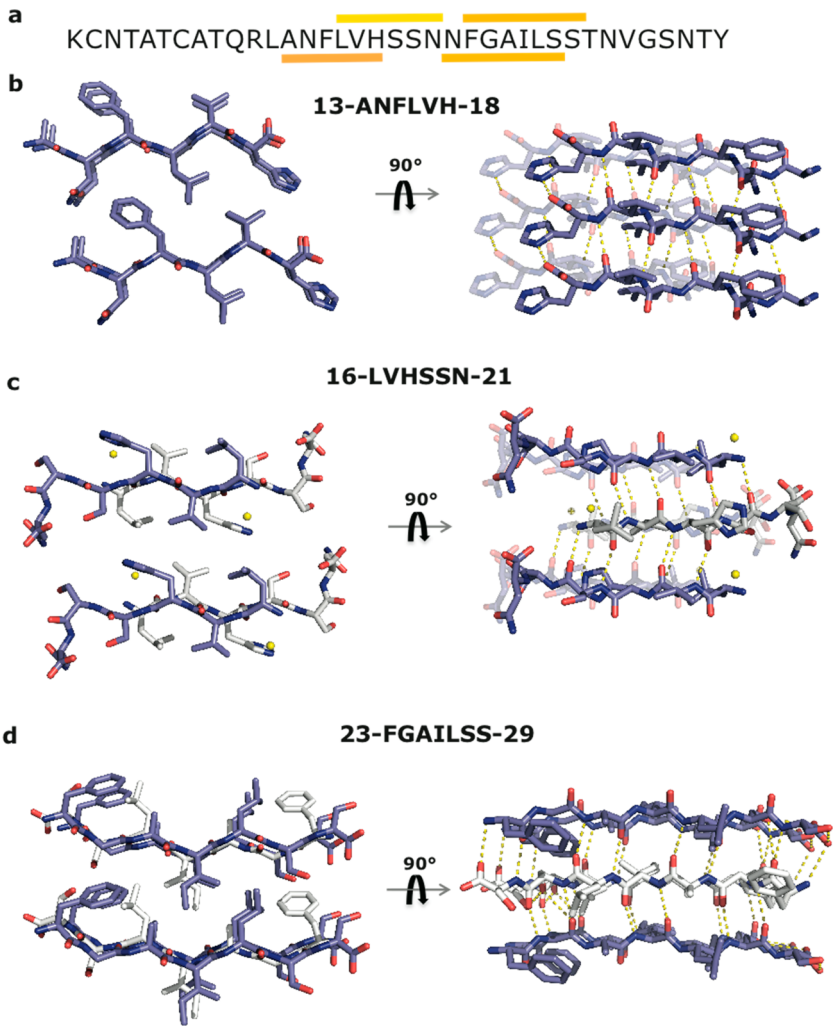

Figure 1. IAPP segments 13-ANFLVH-18, 16-LVHSSN-21, and 23-FGAILSS-29 form in-register steric zippers. (a) Sequence of human IAPP. Segments characterized in this work are highlighted by a colored bar over the segment. (b) Crystal structure of segment ANFLVH. View looking down the fibril axis reveals the steric zipper interface involving phenylalanine, leucine, and valine residues. ANFLVH forms a parallel, Class 2 steric zipper,[6] in which the sheets are related by a pure translation. View perpendicular to the fibril axis reveals hydrogen bond network and stacking of aromatic residues Phe and His, which adds to the stability of the zipper. (c) View down the fibril axis showing the steric zipper interface of segment LVHSSN. This peptide forms a Class 7 steric zipper, in which the strands stack with antiparallel orientations, while the sheets pack parallel to each other. View perpendicular to the fibril axis, showing the hydrogen bond network of LVHSSN. There is little interdigitation of side chains. (d) Crystal structure of segment FGAILSS. View down the fibril axis reveals the steric zipper interface. The segment forms a Class 6 steric zipper with the strands in one sheet stacked antiparallel to each other and the two sheets arranged parallel to each other. Water molecules are shown as yellow spheres.

fibrillar state, a phenomenon referred to as polymorphism. Depending upon the conditions, IAPP has been found to form different fibrillar structures varying in their width, pitch length, and ultrastructure.[18,19] Our previous work has proposed the molecular basis of extreme polymorphism seen in IAPP-derived fibrils. We have found multiple pathways that can lead to variant fibril assemblies. In IAPP, we find that the same segment can adopt different steric zippers, a phenomenon that we have previously termed "packing polymorphism". Various segments can also nucleate into different steric zippers, a phenomenon termed "segmental polymorphism".[20,21]

Here we provide additional atomic resolution structures of segments from the fibril core of IAPP previously identified,[21] one of which forms an out-of-register steric zipper.

MATERIALS AND METHODS

Sample Preparation and Crystallization. Peptides were synthesized at >97% purity from CS. Bio (Menlo Park, CA) and Celtek Bioscience (Nashville, TN). All peptide solutions were filtered through a 0.1 μm Ultrafree-MC centrifugal filter device (Amicon, Bedford, MA) prior to crystallization experiments at 18 °C via hanging-drop vapor diffusion. Crystallization was carried out in 24-well plates with 1 mL reservoir solution and 1 to 1.5 uL peptide/reservoir drop sizes.

Crystallization Conditions. *13-ANFLVH-18.* This segment was dissolved at 20 mg/mL in water and mixed with 10% (w/v) PEG-8000, 0.1 M Na/K phosphate pH 6.2, and 0.2 M NaCl at a 1:1 ratio by volume. Needle-like crystals appeared within 24 h.

16-LVHSSN-21. This segment was dissolved at 20 mg/mL in water and mixed with 0.09 M HEPES pH 7.5, 1.26 M trisodium

DOI: 10.1021/acs.jpcb.5b09981
J. Phys. Chem. B XXXX, XXX, XXX−XXX

Table 1. Statistics of Structure Determination of Four Segments of IAPP That Form Steric Zippers[a]

	13-ANFLVH-18	16-LVHSSN-21	22-NFGAILS-28	23-FGAILSS-29
		Crystal Parameters		
Cell dimensions				
space group	$P2_1$	$P2_1$	$P1$	$P1$
a, *b*, *c* (Å)	4.8, 39.7, 9.9	9.6, 9.6, 19.0	8.66, 11.6, 21.6	8.8, 9.5, 24.7
α, β, γ (deg)	90.0, 103.7, 90.0	90.0, 101.2, 90.0	86.4, 82.2, 76.4	88.2, 80.0, 70.3
molecules in asymmetric unit	1	1	1	1
		Data Collection		
synchrotron beamline	APS (24-ID-E)	APS (24-ID-E)	APS (24-ID-E)	APS (24-ID-E)
wavelength (Å)	0.9792	0.9792	0.9792	0.9792
resolution (Å)	1.61	1.66	1.24	1.78
unique reflections	433	391	2227	647
overall redundancy	3.1 (3.2)	3.0(3.0)	2.9(2.6)	5.2(4.0)
completeness (%)	93.8 (87.0)	90.6 (97.1)	97.8 (96.9)	93.4 (72.3)
Rmerge (%)[b]	14.7 (13.3)	7.6 (14.9)	16.6 (55.8)	24.1 (69.6)
$\langle I/\sigma_I \rangle$	6.6 (9.7)	14.1 (9.1)	6.5 (1.6)	4.3 (1.4)
		Refinement		
resolution (Å)	19.86−1.61	19.53−1.66	21.34−1.24	24.35−1.78
Rwork (%)[c]	11.2	16.7	17.3	16.7
Rfree (%)[d]	16.1	19.8	20.6	21.8
no. atoms				
protein	50	46	102	98
ligand/ion	0	0	0	0
water	0	1	7	0
overall B factors	7.8	4.6 (4.4[e])	2.3 (1.9[e])	23.7
rms deviation				
bond length (Å)	0.003	0.004	0.008	0.016
bond angle (deg)	0.70	1.0	1.0	2.0

[a]Values in parentheses correspond to the highest resolution shell. [b]$Rmerge = \Sigma|I - \langle I \rangle|/\Sigma I$. [c]$Rwork = \Sigma|F_o - F_c|/\Sigma F_o$. [d]$Rfree = \Sigma|F_o - F_c|/\Sigma F_o$, calculated using a random set containing 10% reflections that were not included throughout structure refinement. [e]Without water.

Table 2. Structural Characteristics of the Four Steric Zippers Determined in This Work

segment	zipperDB[a] (kcal/mol)	strand orientation	steric zipper class	area buried (Å^2)[b]	shape complementarity[c]
13-ANFLVH-18	−22.900	parallel	face-to-back in register β-sheets symmetry class 2	258	0.80
16-LVHSSN-21	−22.000	antiparallel	face-to-back staggered β-sheets symmetry class 7	160	0.50
22-NFGAILS-28	−22.300	antiparallel	face-to-back out of register β-sheets symmetry class 7	293	0.83
23-FGAILSS-29	−22.500	antiparallel	face-to-back in register symmetry class 6	217	0.77

[a]Estimated energies of steric zippers formed by six-residue segments (starting at the listed residue) of IAPP. Segments having energies of −23 kcal mol^{-1} or lower are predicted to form fibrils.[28] [b]Area buried was calculated using AREAIMOL[43] with a probe radius of 1.4 Å. The summation of the difference between the accessible surface areas of (a) one β-strand alone and in contact with the opposite β-sheet and (b) the β-sheet alone and in contact with the opposite β-strand, constitutes the reported area buried. In structures with antiparallel β-strand orientation, as well as in parallel β-strand orientations with different conformations, the average area buried per β-strand is reported. [c]Lawrence and Colman's shape complementarity index.[44]

citrate, and 10% glycerol at a 1:1 ratio by volume. Needle-like crystals appeared in 2 to 3 days.

22-NFGAILS-28. This segment was dissolved at 7 mg/mL in water and mixed with 10% ethanol and 1.5 M NaCl at a 1:1 ratio by volume. Needle-like crystals appeared in 1 week.

23-FGAILSS-29. This segment was dissolved at 6.4 mg/mL in 20 mM lithium hydroxide and mixed with 0.1 M HEPES pH 6.5 and 0.5 M sodium formate at a 2:1 ratio by volume. Short microcrystals appeared in a month.

Data Collection and Structure Refinement. Crystals of IAPP segments ANFLVH, LVHSSN, and NFGAILS were mounted on 20−50 μm Mitegen LD (Ithaca, NY) loops in the presence of 20% glycerol and flash-cooled in liquid nitrogen. Crystals of FGAILSS were mounted on pulled glass capillaries without any cryoprotectant. Data were collected at 100 K using a microfocus beam (5 × 5 μm^2) at beamline 24-ID-E of the Advanced Photon Source (APS) at Argonne National Laboratory. Data indexing, integration, and scaling were performed using XDS/XSCALE and DENZO/SCALEPACK.[22] The merged scaled data were imported into the CCP4 format with programs from the CCP4 program suite organized under the "CCP4i" interface.[23] Molecular replacement solutions for the segments were obtained using the program PHASER,[24] using a polyalanine β strand as the search model. Crystallographic refinements were performed with REFMAC5 and PHENIX.[25] Model building was performed with COOT[26] and illustrated with PyMOL.[27]

RESULTS

In Register Steric Zipper Structures from IAPP. Previously we have shown that full-length IAPP is capable of forming at least two different fibril morphologies that originate

DOI: 10.1021/acs.jpcb.5b09981
J. Phys. Chem. B XXXX, XXX, XXX−XXX

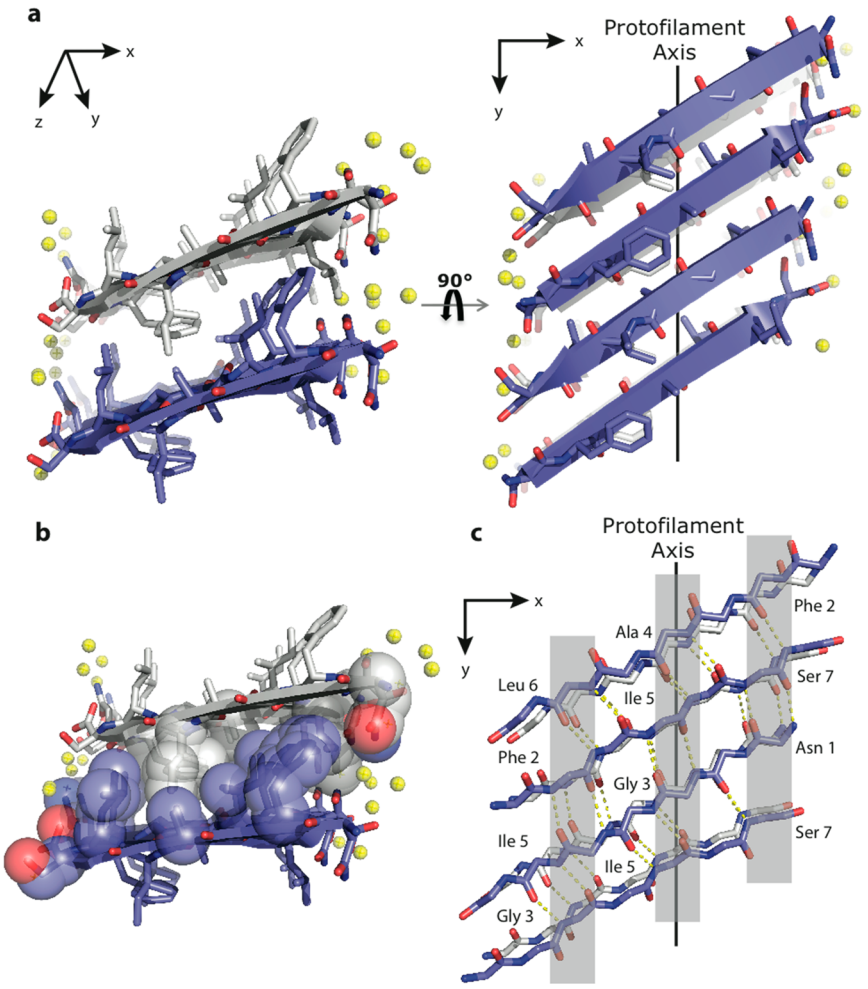

Figure 2. Segment 22-NFGAILS-28 from IAPP forms an out-of-register steric zipper. (a) View looking down the fibril axis shows mating sheets with side chain interdigitation. Right panel shows the view rotated 90° to the fibril axis. The sheets form an acute angle with the protofilament axis as opposed to being exactly perpendicular as seen in in-register steric zippers. Water molecules are shown as yellow spheres. (b) View down the fibril axis with side chains in space filling representation shows the dry interface with mating side chains of Ile and Phe (c) Intrasheet main chain hydrogen bonding along one β sheet. The strands are sheared such that different amino acids line up over each other along the fibril axis (highlighted in gray) in contrast to in-register zippers where the strands align such that the same amino acid residues lie over each other.

from distinct regions within the sequence.[20,21] In addition, we determined crystal structures of six segments within residues 14−37 from IAPP, showing the large variety of steric-zipper spines that can form from the full-length sequence. Here we expand on the previous work, elucidating the atomic details of four more IAPP segments that were identified by ZipperDB[28] to have high fibrillation propensity (Figure 1a, Table 2), bringing the total number of molecular structures of IAPP amyloidogenic segments to ten. Data collection and refinement statistics can be found in Table 1 and steric zipper statistics can be found in Table 2. Three segments, located in the central region of the IAPP, crystallize as in-register steric zippers.

The segment ANFLVH (residues 13−18) forms β strands that are arranged as parallel, in-register β sheets, with a dry steric zipper interface displaying a face-to-back orientation of the pair of sheets (Figure 1b). This is a Class 2 steric zipper.[6] The zipper core consists of hydrophobic interactions involving Phe15 and Val17 of one sheet interdigitating with Leu16 of the adjacent sheet. Both the strands and the sheets pack in a parallel orientation, with Phe and His residues stacking on one another along the sheets, adding to the stability of the fibril (Figure 1b).

The hexameric segment LVHSSN (residues 16−21) forms a staggered in-register steric zipper (Figure 1c) in which the strands stack in an antiparallel orientation, while the sheets are oriented parallel. Thus, the segment forms a Class 7 zipper. This staggered arrangement of β strands has been seen previously and can be termed "locally out-of-register".[29,30] The structure is not "globally out-of-register" because there is no continuous shearing of strands along the sheet. Rather, each pair lies directly above the pair below. This steric zipper lacks the tight interdigitation seen in ANFLVH. It contains water molecules between mating sheets, hydrogen-bonded to serine and histidine residues.

The crystal structure of the segment FGAILSS (residues 23−29) reveals a Class 6 steric zipper with β strands arranged antiparallel in a β sheet and the two mating sheets running parallel to each other (Figure 1d). The crystal structure is completely devoid of water molecules, and the interdigitation between mating sheets is made up of Ala25 and Leu29 from one sheet and Ile26 and Ser 28 from the opposing sheet.

Crystal Structure of IAPP22-28 NFGAILS Reveals an Out-of-Register Steric Zipper. We identified a fourth segment NFGAILS from IAPP, located in the very amyloido-

DOI: 10.1021/acs.jpcb.5b09981
J. Phys. Chem. B XXXX, XXX, XXX−XXX

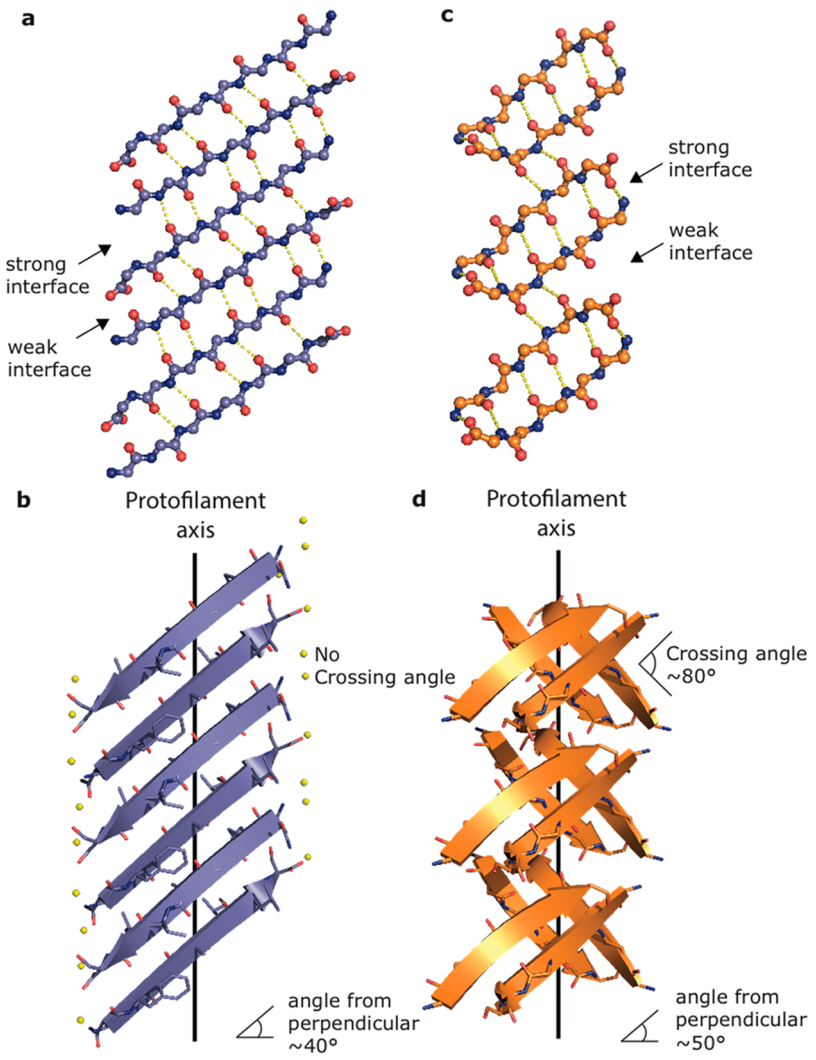

Figure 3. Structural comparison of 22-NFGAILS-28 of IAPP (left) with the previously determined out-of-register steric zipper from β2-microglobulin (right). View of the hydrogen bond network between strands along a single sheet for NFGAILS (a) and KDWSFY (c) (residues 58−63 of β2-microglobulin, PDB 4E0K). The structure of NFGAILS reveals alternating weak and strong interfaces that run along the sheet, in which the weak interface contains five interstrand hydrogen bonds and the strong interface contains six main chain hydrogen bonds. KDWSFY contains a weak interface containing two hydrogen bonds and a strong interface containing six hydrogen bonds. View perpendicular to the fibril axis shows the β sheets of NFGAILS (b) forming an acute angle with the fibril axis similar to KDWSFY (d). However, the sheets completely eclipse each other in NFGAILS, whereas they form an acute angle in KDWSFY.

genic C-terminal region that, interestingly, forms an out-of-register steric zipper (Figure 2a). The segment forms antiparallel β strands arranged into parallel sheets, forming a Class 7 steric zipper. The glycine and alanine residues in the center of the segment allow space for the larger phenylalanine, leucine, and isoleucine residues forming the dry, highly complementary steric-zipper interface (Figure 2b). Each strand within each sheet of NFGAILS is sheared out of register by two residues (Figure 2c), as in the previously determined steric zipper structure from β2m, with KDWSFY (residues 58−63) forming alternate weak and strong hydrogen bonded interfaces (Figure 3a,c).[11] Similar to the KDWSFY structure, the β-strands in the NFGAILS structure are not perpendicular to the fibril axis as in in-register steric zippers;[11] instead, each strand forms an angle of 40° from the perpendicular (Figure 3b,d). Additionally, similar to the previously determined out-of-register structures, NFGAILS also displays alternating weak and strong hydrogen-bonding interfaces. In contrast with β2m structure, the β sheets in NFGAILS have no crossing angle with each other and instead run parallel to each other (Figure 3b,d). This is the first out-of-register structure determined in which the strands completely eclipse each other with a zero crossing angle.

DISCUSSION

Conformational polymorphism has been hypothesized to be the molecular basis of prion strains. Replication of strains upon the addition of new monomers was first reported for the PrP protein, and there is increasing evidence that other amyloid-forming proteins share characteristics of strains, replication, and transmission.[31−36] In our previous work, we showed the atomic basis of polymorphism in IAPP by determining the crystal structures of six amyloidogenic segments that formed different steric zippers.[20,21] The high degree of segmental polymorphism in IAPP is further highlighted in our current work as the different segments characterized here, even when shifted by only one residue from a previously studied segment, form a different class of steric zipper.

DOI: 10.1021/acs.jpcb.5b09981
J. Phys. Chem. B XXXX, XXX, XXX−XXX

The atomic structures of ANFLVH and LVHSSN determined here further support the role of histidine 18 in promoting fibril formation. Mouse IAPP, which does not aggregate, forms abundant fibrils when a single-point replacement R18H is introduced.[21] From the ANFLVH structure, we deduce that the pi stacking of His18 side chains along each sheet contributes to the stability of the fibril that may be one factor that contributes to mouse IAPP R18H mutant fibrillizing.

The crystal structures of FGAILSS and NFGAILS located in the amyloidogenic core of IAPP reveal antiparallel zippers. In our previous work, the atomic structure of AILSST, a segment in which four residues overlap with NFGAILS, was also shown to be an antiparallel zipper.[21] Together the three structures suggest a propensity of the fibril core of IAPP to form antiparallel β sheets, consistent with some models proposed for the packing of amyloidogenic core of IAPP fibrils.[19,37,38] Interestingly, structural studies of another amyloid protein, Abeta, suggest that the fibril core of some of its polymorphs and sequence variants are also composed of antiparallel β sheets.[39−41] It has been proposed that because antiparallel fibrils are typically less stable than parallel fibrils, conversion to potentially toxic, transient morphologies is more likely;[42] however, the physiological consequence of these various fibril architectures is still unclear.

Models of toxic amyloid oligomers and fibrils have emerged from structural studies of cylindrin, amyloid β-sheet mimics (BAMs), and a hexameric segment from β2-microglobulin (β2m).[10−12] A notable characteristic shared in all of these structures is that they are composed of out-of-register β strands. This is in contrast with the classic in-register β-sheet packing seen in most amyloid fibrils.[10−12] The structure of NFGAILS presented here suggests that IAPP may also be capable of forming out-of-register fibrils and oligomers.

The structure of NFGAILS reveals several conserved features with previously determined out-of-register structures. First, in all out-of-register structures determined so far including NFGAILS, the β sheets form an acute angle with the protofilament axis. Second, the β sheets are composed of two interfaces of interstrand hydrogen bond networks: (i) a strong interface in which the hydrogen bond donors and acceptors within the peptide backbone are satisfied and (ii) a weak interface that leaves unsatisfied donors and acceptors. This is notable in the crystal structure of KDWSFY from β2-microglobulin, the only other solved out-of-register fibril structure to date (Figure 3c). The structure of NFGAILS also reveals a moderately weak interface, differing by one hydrogen bond (Figure 3a). One difference between NFGAILS and previously determined out of register zippers is the crossing angle of the mating β sheets. The β sheets in NFGAILS are parallel and do not cross with each other (Figure 3b). In KDWSFY, the sheets form an 80° crossing angle (Figure 3c). While it remains to be determined how these characteristics affect the biological properties of these proteins, nevertheless it highlights the variety of different conformations amyloid segments adopt.

We have further characterized the segments of the fibril core of IAPP, a protein associated with type 2 diabetes, by crystallizing several of its overlapping segments. Our work provides additional evidence that the fibril cores of IAPP are derived from two distinct regions: one involving Histidine18 and the other, more amyloidogenic region, involving residues 20−29. Furthermore, we show that a segment within residues 20−29 can form an antiparallel out-of-register zipper, suggesting that out-of-register zippers may be a common motif in amyloid proteins.

AUTHOR INFORMATION

Corresponding Author

*Fax: (310) 206-3914. E-mail: david@mbi.ucla.edu.

Notes

The authors declare no competing financial interest.

ACKNOWLEDGMENTS

We thank Michael Collazo and beamline staff at the Advanced Photon Source (APS) Northeastern Collaborative Access Team beamline 24-ID-E for help with experiments. The beamline is funded by the National Institute of General Medical Sciences (P41 GM103403) and U.S. Department of Energy (DOE) Office of Science under Contract No. DE-AC02-06CH11357. We thank HHMI, DOE, and NIH AG 029430 for funding. A.B.S. was supported by the UCLA Dissertation Year fellowship and S.S. was supported by the Whitcome predoctoral fellowship. Atomic coordinates and structure factors have been deposited in the Protein Data Bank as 5E5V for NFGAILS, 5E5Z for LVHSSN, 5E61 for FGAILSS, and 5E5X for ANFLVH.

REFERENCES

(1) Eisenberg, D.; Jucker, M. The Amyloid State of Proteins in Human Diseases. *Cell* **2012**, *148*, 1188−1203.

(2) Chiti, F.; Dobson, C. M. Protein Misfolding, Functional Amyloid, and Human Disease. *Annu. Rev. Biochem.* **2006**, *75*, 333−366.

(3) Xu, J.; Reumers, J.; Couceiro, J. R.; De Smet, F.; Gallardo, R.; Rudyak, S.; Cornelis, A.; Rozenski, J.; Zwolinska, A.; Marine, J.-C.; et al. Gain of Function of Mutant p53 by Coaggregation with Multiple Tumor Suppressors. *Nat. Chem. Biol.* **2011**, *7*, 285−295.

(4) Makin, O. S.; Serpell, L. C. Structures for Amyloid Fibrils: Structures for Amyloid Fibrils. *FEBS J.* **2005**, *272*, 5950−5961.

(5) Nelson, R.; Sawaya, M. R.; Balbirnie, M.; Madsen, A. Ø.; Riekel, C.; Grothe, R.; Eisenberg, D. Structure of the Cross-B Spine of Amyloid-like Fibrils. *Nature* **2005**, *435*, 773−778.

(6) Sawaya, M. R.; Sambashivan, S.; Nelson, R.; Ivanova, M. I.; Sievers, S. A.; Apostol, M. I.; Thompson, M. J.; Balbirnie, M.; Wiltzius, J. J. W.; McFarlane, H. T.; et al. Atomic Structures of Amyloid Cross-B Spines Reveal Varied Steric Zippers. *Nature* **2007**, *447*, 453−457.

(7) Glabe, C. G. Structural Classification of Toxic Amyloid Oligomers. *J. Biol. Chem.* **2008**, *283*, 29639−29643.

(8) Haass, C.; Selkoe, D. J. Soluble Protein Oligomers in Neurodegeneration: Lessons from the Alzheimer's Amyloid B-Peptide. *Nat. Rev. Mol. Cell Biol.* **2007**, *8*, 101−112.

(9) Laganowsky, A.; Liu, C.; Sawaya, M. R.; Whitelegge, J. P.; Park, J.; Zhao, M.; Pensalfini, A.; Soriaga, A. B.; Landau, M.; Teng, P. K.; et al. Atomic View of a Toxic Amyloid Small Oligomer. *Science* **2012**, *335*, 1228−1231.

(10) Liu, C.; Sawaya, M. R.; Cheng, P.-N.; Zheng, J.; Nowick, J. S.; Eisenberg, D. Characteristics of Amyloid-Related Oligomers Revealed by Crystal Structures of Macrocyclic B-Sheet Mimics. *J. Am. Chem. Soc.* **2011**, *133*, 6736−6744.

(11) Liu, C.; Zhao, M.; Jiang, L.; Cheng, P.-N.; Park, J.; Sawaya, M. R.; Pensalfini, A.; Gou, D.; Berk, A. J.; Glabe, C. G.; et al. Out-of-Register -Sheets Suggest a Pathway to Toxic Amyloid Aggregates. *Proc. Natl. Acad. Sci. U. S. A.* **2012**, *109*, 20913−20918.

(12) Cheng, P.-N.; Liu, C.; Zhao, M.; Eisenberg, D.; Nowick, J. S. Amyloid B-Sheet Mimics That Antagonize Protein Aggregation and Reduce Amyloid Toxicity. *Nat. Chem.* **2012**, *4*, 927−933.

(13) Cooper, G. J. S.; Willis, A. C.; Clark, A.; Turner, R. C.; Sim, R. B.; Reid, K. B. M. Purification and Characterization of a Peptide from

DOI: 10.1021/acs.jpcb.5b09981
J. Phys. Chem. B XXXX, XXX, XXX−XXX

Amyloid-Rich Pancreases of Type 2 Diabetic Patients. *Proc. Natl. Acad. Sci. U. S. A.* **1987**, *84*, 8628−8632.
(14) Westermark, P.; Wernstedt, C.; Wilander, E.; Sletten, K. A Novel Peptide in the Calcitonin Gene Related Peptide Family as an Amyloid Fibril Protein in the Endocrine Pancreas. *Biochem. Biophys. Res. Commun.* **1986**, *140*, 827−831.
(15) Kahn, S. E.; Andrikopoulos, S.; Verchere, C. B. Islet Amyloid: A Long-Recognized but Underappreciated Pathological Feature of Type 2 Diabetes. *Diabetes* **1999**, *48*, 241−253.
(16) Cao, P.; Marek, P.; Noor, H.; Patsalo, V.; Tu, L.-H.; Wang, H.; Abedini, A.; Raleigh, D. P. Islet Amyloid: From Fundamental Biophysics to Mechanisms of Cytotoxicity. *FEBS Lett.* **2013**, *587*, 1106−1118.
(17) Tenidis, K.; Waldner, M.; Bernhagen, J.; Fischle, W.; Bergmann, M.; Weber, M.; Merkle, M.-L.; Voelter, W.; Brunner, H.; Kapurniotu, A. Identification of a Penta- and Hexapeptide of Islet Amyloid Polypeptide (IAPP) with Amyloidogenic and Cytotoxic Properties. *J. Mol. Biol.* **2000**, *295*, 1055−1071.
(18) Goldsbury, C. S.; Cooper, G. J. S.; Goldie, K. N.; Muller, S.; Saafi, E. L.; Gruijters, W. T. M.; Misur, M. P.; Engel, A.; Aebi, U.; Kistler, J. Polymorphic Fibrillar Assembly of Human Amylin. *J. Struct. Biol.* **1997**, *119*, 17−27.
(19) Madine, J.; Jack, E.; Stockley, P. G.; Radford, S. E.; Serpell, L. C.; Middleton, D. A. Structural Insights into the Polymorphism of Amyloid-Like Fibrils Formed by Region 20−29 of Amylin Revealed by Solid-State NMR and X-ray Fiber Diffraction. *J. Am. Chem. Soc.* **2008**, *130*, 14990−15001.
(20) Wiltzius, J. J. W.; Sievers, S. A.; Sawaya, M. R.; Cascio, D.; Popov, D.; Riekel, C.; Eisenberg, D. Atomic Structure of the Cross-B Spine of Islet Amyloid Polypeptide (amylin). *Protein Sci.* **2008**, *17*, 1467−1474.
(21) Wiltzius, J. J. W.; Landau, M.; Nelson, R.; Sawaya, M. R.; Apostol, M. I.; Goldschmidt, L.; Soriaga, A. B.; Cascio, D.; Rajashankar, K.; Eisenberg, D. Molecular Mechanisms for Protein-Encoded Inheritance. *Nat. Struct. Mol. Biol.* **2009**, *16*, 973−978.
(22) Kabsch, W. Automatic Processing of Rotation Diffraction Data from Crystals of Initially Unknown Symmetry and Cell Constants. *J. Appl. Crystallogr.* **1993**, *26*, 795−800.
(23) The CCP4 Suite: Programs for Protein Crystallography. *Acta Crystallogr., Sect. D: Biol. Crystallogr.* **1994**, *50*, 760−763 10.1107/S0907444994003112.
(24) Read, R. J. Pushing the Boundaries of Molecular Replacement with Maximum Likelihood. *Acta Crystallogr., Sect. D: Biol. Crystallogr.* **2001**, *57*, 1373−1382.
(25) Adams, P. D.; Afonine, P. V.; Bunkóczi, G.; Chen, V. B.; Davis, I. W.; Echols, N.; Headd, J. J.; Hung, L.-W.; Kapral, G. J.; Grosse-Kunstleve, R. W.; et al. *PHENIX*: A Comprehensive Python-Based System for Macromolecular Structure Solution. *Acta Crystallogr., Sect. D: Biol. Crystallogr.* **2010**, *66*, 213−221.
(26) Emsley, P.; Cowtan, K. *Coot*: Model-Building Tools for Molecular Graphics. *Acta Crystallogr., Sect. D: Biol. Crystallogr.* **2004**, *60*, 2126−2132.
(27) *The PyMOL Molecular Graphics System*, version 1.5.0.4, Schrödinger, LLC.
(28) Goldschmidt, L.; Teng, P. K.; Riek, R.; Eisenberg, D. Identifying the Amylome, Proteins Capable of Forming Amyloid-like Fibrils. *Proc. Natl. Acad. Sci. U. S. A.* **2010**, *107*, 3487−3492.
(29) Mehta, A. K.; Lu, K.; Childers, W. S.; Liang, Y.; Dublin, S. N.; Dong, J.; Snyder, J. P.; Pingali, S. V.; Thiyagarajan, P.; Lynn, D. G. Facial Symmetry in Protein Self-Assembly. *J. Am. Chem. Soc.* **2008**, *130*, 9829−9835.
(30) Liang, Y.; Pingali, S. V.; Jogalekar, A. S.; Snyder, J. P.; Thiyagarajan, P.; Lynn, D. G. Cross-Strand Pairing and Amyloid Assembly. *Biochemistry* **2008**, *47*, 10018−10026.
(31) Prusiner, S. B. A Unifying Role for Prions in Neurodegenerative Diseases. *Science* **2012**, *336*, 1511−1513.
(32) Brundin, P.; Melki, R.; Kopito, R. Prion-like Transmission of Protein Aggregates in Neurodegenerative Diseases. *Nat. Rev. Mol. Cell Biol.* **2010**, *11*, 301−307.
(33) Lu, J.-X.; Qiang, W.; Yau, W.-M.; Schwieters, C. D.; Meredith, S. C.; Tycko, R. Molecular Structure of B-Amyloid Fibrils in Alzheimer's Disease Brain Tissue. *Cell* **2013**, *154*, 1257−1268.
(34) Masuda-Suzukake, M.; Nonaka, T.; Hosokawa, M.; Oikawa, T.; Arai, T.; Akiyama, H.; Mann, D. M. A.; Hasegawa, M. Prion-like Spreading of Pathological -Synuclein in Brain. *Brain* **2013**, *136*, 1128−1138.
(35) Sanders, D. W.; Kaufman, S. K.; DeVos, S. L.; Sharma, A. M.; Mirbaha, H.; Li, A.; Barker, S. J.; Foley, A. C.; Thorpe, J. R.; Serpell, L. C.; et al. Distinct Tau Prion Strains Propagate in Cells and Mice and Define Different Tauopathies. *Neuron* **2014**, *82*, 1271−1288.
(36) Marshall, K. E.; Serpell, L. C. Fibres, Crystals and Polymorphism: The Structural Promiscuity of Amyloidogenic Peptides. *Soft Matter* **2010**, *6*, 2110.
(37) Ashburn, T. T.; Auger, M.; Lansbury, P. T. The Structural Basis of Pancreatic Amyloid Formation: Isotope-Edited Spectroscopy in the Solid State. *J. Am. Chem. Soc.* **1992**, *114*, 790−791.
(38) Griffiths, J. M.; Ashburn, T. T.; Auger, M.; Costa, P. R.; Griffin, R. G.; Lansbury, P. T. Rotational Resonance Solid-State NMR Elucidates a Structural Model of Pancreatic Amyloid. *J. Am. Chem. Soc.* **1995**, *117*, 3539−3546.
(39) Lansbury, P. T.; Costa, P. R.; Griffiths, J. M.; Simon, E. J.; Auger, M.; Halverson, K. J.; Kocisko, D. A.; Hendsch, Z. S.; Ashburn, T. T.; Spencer, R. G. S.; et al. Structural Model for the B-Amyloid Fibril Based on Interstrand Alignment of an Antiparallel-Sheet Comprising a C-Terminal Peptide. *Nat. Struct. Biol.* **1995**, *2*, 990−998.
(40) Colletier, J.-P.; Laganowsky, A.; Landau, M.; Zhao, M.; Soriaga, A. B.; Goldschmidt, L.; Flot, D.; Cascio, D.; Sawaya, M. R.; Eisenberg, D. Molecular Basis for Amyloid-B Polymorphism. *Proc. Natl. Acad. Sci. U. S. A.* **2011**, *108*, 16938−16943.
(41) Qiang, W.; Yau, W.-M.; Luo, Y.; Mattson, M. P.; Tycko, R. Antiparallel -Sheet Architecture in Iowa-Mutant -Amyloid Fibrils. *Proc. Natl. Acad. Sci. U. S. A.* **2012**, *109*, 4443−4448.
(42) Berthelot, K.; Ta, H. P.; Géan, J.; Lecomte, S.; Cullin, C. In Vivo and In Vitro Analyses of Toxic Mutants of HET-S: FTIR Antiparallel Signature Correlates with Amyloid Toxicity. *J. Mol. Biol.* **2011**, *412*, 137−152.
(43) Lee, B.; Richards, F. M. The Interpretation of Protein Structures: Estimation of Static Accessibility. *J. Mol. Biol.* **1971**, *55*, 379−IN4.
(44) Lawrence, M. C.; Colman, P. M. Shape Complementarity at Protein/Protein Interfaces. *J. Mol. Biol.* **1993**, *234*, 946−950.

DOI: 10.1021/acs.jpcb.5b09981
J. Phys. Chem. B XXXX, XXX, XXX−XXX